~~N-10890~~ Copy 180

[redacted]

NASA TM X-481

NASA TM X-481

GPO PRICE $

CFSTI PRICE(S) $

Hard copy (HC) 2.00

Microfiche (MF) .50

ff 653 July 65

DECLASSIFIED- US: 1688
TAINE TO ROBERTSON MEMO
DATED 9/28/66

Declassified by authority of NASA
Classification Change Notices No.
Dated ** 10/12/66

TECHNICAL MEMORANDUM

X-481

INVESTIGATION OF EIGHT-STAGE BLEED-TYPE TURBINE FOR HYDROGEN-PROPELLED NUCLEAR ROCKET APPLICATIONS

II - EXPERIMENTAL OVERALL AND STAGE GROUP PERFORMANCE DETERMINED IN COLD NITROGEN

[redacted]

By Harold E. Rohlik

Lewis Research Center
Cleveland, Ohio

AUTHORITY
Ltr NASA, Dtd 12 Nov 62, Sub: Aut... Time Phased Downgrading & Declass... System. Signed H. G. Maines, Code ...

N66 39612
(ACCESSION NUMBER)

(THRU)

36
(PAGES)

1
(CODE)

TMX-481
(NASA CR OR TMX OR AD NUMBER)

22
(CATEGORY)

FACILITY FORM 602

[redacted]

NATIONAL AERONAUTICS AND SPACE ADMINISTRATION

WASHINGTON [redacted] March 1962

[redacted]

1V

DECLASSIFIED- US: 1688
TAINE TO ROBERTSON MEMO
[redacted] 9/28/66

E-1454

NATIONAL AERONAUTICS AND SPACE ADMINISTRATION

TECHNICAL MEMORANDUM X-481

INVESTIGATION OF EIGHT-STAGE BLEED-TYPE TURBINE FOR HYDROGEN-PROPELLED NUCLEAR ROCKET APPLICATIONS

II - EXPERIMENTAL OVERALL AND STAGE GROUP PERFORMANCE DETERMINED IN COLD NITROGEN*

By Harold E. Rohlik

Declassified by authority of NASA Classification Change Notices No. 80 Dated ** 10/12/66

SUMMARY

Performance characteristics of an eight-stage turbine designed for the turbopump of a hydrogen-propelled nuclear rocket were investigated experimentally in cold nitrogen. At design speed and overall turbine total-to-static pressure ratio the overall total efficiency was 0.67 (design or predicted efficiency was 0.75), with 0.68 in the first stage and 0.57 to 0.62 in all other stages. This difference resulted largely from the lower reaction and higher turning in stators of all stages after the first stage. Examination of design characteristics and experimental performance of this and other turbines indicates that improvements in efficiency could be obtained through improved tip clearance geometry and lower rotor blade surface diffusion.

INTRODUCTION

The turbopump system of a high-pressure bleed-type hydrogen-propelled nuclear rocket requires relatively high turbine flow rates to provide the required pumping power. Since turbine flow reduces the effective rocket specific impulse, it is desirable to minimize turbine flow by providing high turbine efficiencies. Reference 1 describes turbopumps suitable for this application and shows that multistage turbines are required to achieve the relatively high efficiencies required to minimize the specific impulse penalty.

The design of an eight-stage turbine for this application and the experimental performance of the first two stages are described in reference 2. In the investigation reported in reference 2, the first two

*Title, Unclassified.

[redacted]

[redacted]

[redacted]

stages were tested over a range of speeds and pressure ratios in cold hydrogen and cold nitrogen. Turbine performance was the same in both gases when adjusted to standard air. Subsequently, four-, six-, and eight-stage assemblies have been tested in cold nitrogen at the Plum Brook Rocket Systems Research Facility. This report presents overall and stage group performance as obtained from these tests.

SYMBOLS

E-1454

c_p	specific heat at constant pressure, Btu/(lb)($^{\circ}$R)
g	acceleration due to gravity, 32.17 ft/sec^2
$\Delta h'$	turbine specific work, Btu/lb
J	mechanical equivalent of work, 778.2 ft-lb/Btu
N	rotative speed, rpm
p	pressure, lb/sq ft
R	gas constant, 766.5 in hydrogen, 55.16 in nitrogen, ft-lb/(lb)($^{\circ}$R)
T	temperature, $^{\circ}$R
U	mean blade velocity, ft/sec
V	absolute gas velocity, ft/sec
V_{cr}	critical velocity, $\sqrt{\frac{2\gamma gRT'}{\gamma + 1}}$, ft/sec
V_j	ideal jet speed corresponding to turbine pressure ratio, $\sqrt{2gJc_pT_i'\left[1 - (p_e/p_i')^{\frac{\gamma-1}{\gamma}}\right]}$
w	weight flow, lb/sec
γ	ratio of specific heats
δ	ratio of inlet pressure to NACA sea-level pressure, $p_i'/2116.2$

[redacted]

ϵ function of γ used in relating weight flow to that using inlet conditions at NACA standard sea-level atmosphere,

$$0.740 \, \frac{1}{\gamma}\left(\frac{\gamma + 1}{2}\right)^{\frac{\gamma}{\gamma - 1}}$$

η turbine efficiency based on inlet and exit total pressures

η_s turbine efficiency based on inlet total and exit static pressures

θ_{cr} squared ratio of turbine-inlet critical velocity to that of NACA standard sea-level atmosphere, $\left(\frac{V_{cr}}{1019}\right)^2$

ν ratio of mean blade speed to ideal jet speed, U/V_j

τ torque parameter, ratio of change in whirl velocity to ideal jet speed, $\Delta V_u/V_j$

Subscripts:

e exit

eq equivalent

i inlet

id ideal

u circumferential component

Superscript:

' absolute total state

DESCRIPTION OF TURBINE

As described in reference 2, the turbine was designed to drive a 100-pound-per-second liquid-hydrogen pump at 47,800 rpm and a pressure rise of 1390 pounds per square inch. The turbine design parameters resulting from these requirements and a turbine design study are reproduced from reference 2 as follows:

E-1454

Hydrogen weight flow, w, lb/sec	3.475
Specific work, $\Delta h'$, Btu/lb	2394
Mean blade speed, U, ft/sec	1420
Blade-jet speed ratio, ν	0.110
Static efficiency, η_s	0.72
Turbine pressure ratio, p_i'/p_e	12.68
Mean diameter, in.	6.81

The design turbine-inlet conditions of 1000 pounds per square inch and 1860° R in hydrogen result in the following parameters used to adjust design numbers to equivalent air:

$$\theta_{cr} = 51.22 \qquad \delta = 68.05$$

$$\sqrt{\theta_{cr}} = 7.157 \qquad \epsilon = 1.012$$

These parameters were selected so that all experimental data could be reduced to a common standard regardless of gas or inlet gas conditions. Design parameters reduced to standard air are as follows for the various stage groups tested:

Parameter	First stage	First two stages	First four stages	First six stages	Eight stages
Weight flow, $\frac{w\sqrt{\theta_{cr}}}{\delta}\epsilon$, lb/sec	0.370	0.370	0.370	0.370	0.370
Specific work, $\Delta h'/\theta_{cr}$, Btu/lb	5.84	11.68	23.36	35.04	46.72
Rotative speed, $N/\sqrt{\theta_{cr}}$, rpm	6679	6679	6679	6679	6679
Pressure ratio, $(p_i'/p_e)_{eq}$	1.326	1.730	3.102	6.064	13.25
Blade-jet speed ratio, ν	.284	.208	.151	.125	.110
Total efficiency, η	.689	.695	.712	.730	.749

A photograph of the turbine rotor is shown in figure 1.

APPARATUS AND INSTRUMENTATION

The test facility and instrumentation used in the subject investigation were the same as those described in reference 2. The test rig supporting the turbine itself was different, however, and included the eight-stage casing and bearing support designed for hot operation. This test setup is shown in figure 2(a). Turbine power was absorbed by the dynamometer directly coupled to the turbine. The change in test equipment was required in order to accommodate additional turbine stages and the resulting higher inlet pressure, torques, and shaft thrusts. Since shaft thrust calculated for design operation of the turbine was considerably larger than the thrust capacity of the ball bearings, a thrust balance system was incorporated. This system employs areas on the shaft that are loaded on one side from the space upstream of the first rotor and on the other side from the turbine exhaust, as shown in figure 2(b). The areas were sized to provide zero shaft thrust at design operation. The compensating force thus provided is always directly proportional to the pressure differential across the turbine rotor assembly. It was assumed that the shaft thrust, which also results from this differential as it acts across the rotors and seals, also remains proportional to the rotor pressure differential so that thrust is balanced for all operating conditions, with the capacity of the ball bearings providing a margin of safety. This system was selected because it required no controls.

Labyrinth seals separated the high- and low-pressure spaces in the turbine. Leakage flow passing through these seals was measured with a calibrated venturi in the thrust balance line. This flow was then subtracted from the flow measured in the turbine-inlet pipe in order to determine the flow passing through the turbine.

EXPERIMENTAL PROCEDURE

Test data were recorded on magnetic tape with high-speed digital equipment for steady-state operation in cold nitrogen over a range of speeds and pressure ratios. Low-pressure-ratio data were obtained with an inlet pressure of 100 pounds per square inch absolute, while high-pressure-ratio data were run with atmospheric exhaust and inlet pressures up to 200 pounds per square inch absolute. Zero-speed torque and weight-flow measurements were made over a range of pressure ratios for four-, six-, and eight-stage operation.

RESULTS AND DISCUSSION

Efficiency

Figure 3 shows the variation in overall total efficiency with blade-jet speed ratio for each group of stages tested, including one and two stages reproduced from reference 2. At their respective design blade-jet speed ratios the efficiencies were 0.67, 0.65, 0.63, 0.66, and 0.67. Design total efficiencies were 0.69, 0.69, 0.71, 0.73, and 0.75, which correspond to a total efficiency of 0.69 in each stage. The experimental efficiencies, as well as all other performance parameters, are based on flow actually passing through all blade rows. Although flow passing through the thrust-balance system represents a loss in turbine performance, the efficiencies presented are the aerodynamic efficiencies more comparable with the design efficiencies.

Figure 4 shows the variation in overall static efficiency with blade-jet speed ratio for eight-stage operation. The efficiency at design blade-jet speed ratio was 0.65. Design static efficiency was 0.72.

The design efficiencies were taken from reference 3, which employed loss coefficients based on experimental performance of several research turbines. Examination of the design characteristics of the subject turbine and the turbines used to determine the loss coefficients of reference 2 showed three major differences that could contribute to the differences between design or "predicted" efficiency and the experimental efficiency of the eight-stage turbine. These were:

(1) The reference turbines were all single-stage units and did not, therefore, incur losses associated with interstage seal leakage or the higher stator blade diffusion in all stages after the first.

(2) The rotor tip clearances of the reference turbines amounted to about 1 percent of the passage height, while in the subject turbine the range was from 7.5 percent in the first stage to 2.6 in the eighth. This difference resulted from the higher hub-tip radius ratios in the subject turbine, 0.80 to 0.92, compared with 0.6 and 0.7, and the "hot" design condition, which included allowances for differential thermal expansion. This accounts for an estimated 0.03 loss in efficiency using the results of reference 4. This loss could be reduced with blades of full passage height and tip clearance recessed in the turbine casing.

(3) The reference turbines were large high-flow machines of the jet-engine type with high through-flow velocities and, consequently, turning angles smaller than in the subject turbine. This difference in turning angles, in combination with the effect of blade trailing-edge thickness relative to turbine diameter, results in lower blockage ratios in the larger turbines. The first stator blockage in the subject turbine was 14.2 percent compared with approximately 4 percent in the reference turbines.

Figure 5 shows the curves of figure 3 superimposed with design efficiencies included. The design overall efficiencies show a steady increase with stage number because of reheat, while each stage has a total efficiency of 0.69. Experimental efficiencies show this trend only in the latter stages. This results from the difference in performance between the first and subsequent stages. Reference 2 reported efficiencies of 0.68 and 0.61 for the first and second stages when operated together at design speed and overall pressure ratio. It appears, therefore, that adding stages results in a lower average efficiency that is offset by the effect of reheat.

It may also be noted from figure 5 that efficiencies appreciably higher than those measured at design blade-jet speed ratio were obtained at higher blade-jet speed ratios. This suggests a design change consisting of more turbine stages in order to reduce stage work and consequently raise the stage blade-jet speed ratios and efficiency level. The significance of turbine efficiency is analyzed in reference 1, wherein figure 10 shows that an increase in turbine efficiency from 0.65 to 0.70 would result in a 2-percent decrease in rocket gross weight for the earth satellite mission considered.

Torque

A dimensionless torque parameter defined as the ratio of change in whirl velocity to ideal jet velocity, $\tau = \dfrac{\Delta V_u}{\sqrt{2gJ\ \Delta h_{id}}} = \dfrac{\eta_s}{2\nu}$, was computed for all data points included in the report. Figure 6 shows that the variation with blade-jet speed ratio for each configuration is nearly linear. The distribution of points near zero speed deviated from the linear variation with higher torque values, which confirms the predicted trends in reference 5. With four, six, and eight stages, zero-speed torque measurements were made at design pressure ratio with the dynamometer rotor locked.

Weight Flow

Figure 7 shows the variation in equivalent flow with speed and pressure ratio for the four-, six-, and eight-stage tests of the subject investigation as well as the two-stage tests reported in reference 2. At design pressure ratios and design speed the equivalent flows were 0.375, 0.377, 0.379, and 0.380 for two, four, six, and eight stages, respectively, while the design flow was 0.370. The excess flow, 1.1 to 2.7 percent, indicates that static pressure at the first stator exit was slightly below the design value. Flow rate is very sensitive to changes in static pressure at the subsonic design flow condition. The design stator-exit critical velocity ratio was 0.54, where a 2-percent excess in flow corresponds to a difference of 0.015 in critical velocity ratio and only 1.0 percent in static pressure.

Only the eight-stage assembly is choked at design speed and pressure ratio. The fact that the other stage groups were not choked makes it possible to use equivalent weight-flow plots at design speed to determine the operating point of each stage group as part of the eight-stage assembly.

The eight-stage turbine was choked at all speeds for pressure ratios greater than 10. Total equivalent weight flow measured at design speed and pressure ratio was 0.386 pound per second, with 0.006 passing through the seals in the thrust balance system and 0.380 through the blade rows. The total flow was 4.3 percent greater than the design value, while the net flow through the blading was 2.7 percent greater than the design value.

E-1454

Performance Maps

Turbine performance maps for two-, four-, six-, and eight-stage operation are shown in figure 8. Contours of total efficiency are plotted for all except the complete turbine, since the kinetic energy leaving is available for subsequent stages. As noted in reference 2, this performance plot was selected because it shows the changes in all variables simultaneously for speed or pressure ratio changes. Points representing design work and weight-flow-speed parameter and also experimental performance at design speed and pressure ratio are shown.

Stage Performance

The weight-flow curves of figure 7 were used to determine the operating conditions of each stage group as a part of the eight-stage turbine. This was done by reading eight-stage weight flow at design speed and pressure ratio in figure 7(d). This value was then used to determine stage group pressure ratio on the design speed lines of figures 7(a) to (c). After determining the operating points of each stage group, interstage total pressures were calculated at the exits of the second, fourth, and sixth stages so that two-stage performance could be determined. Results of this analysis are shown in table I. Stages 1 and 2 show the highest efficiency at 0.64, while the subsequent stage groups ranged from 0.57 to 0.62, averaging 0.60. The overall efficiency of stages 1 and 2, as noted in reference 2, results from stage efficiencies of 0.68 and 0.61, with the difference in stator blade diffusion largely accounting for the difference in efficiencies. Examination of the design characteristics of the various stages showed that rotor-blade loading as indicated by surface velocity diffusion also may have contributed to the differences between stages 1 and 2 and the other two-stage groups. The design values of rotor diffusion were 0.4 in stages 1 and 2 and about 0.6 in each of the other stages. It appears, then, that the stage efficiencies were near 0.60 in all stages except the first, which operated at 0.68.

SUMMARY OF RESULTS

This report has presented the results of the experimental evaluation of an eight-stage turbine designed for a hydrogen-propelled bleed-type nuclear rocket. Design information and experimental performance characteristics of the first two stages have been published previously and are included herein. Results of the investigation can be summarized as follows:

E-1454

1. The total efficiency of the first four stages was 0.63 at the design blade-jet speed ratio of 0.151. The equivalent flow at design operation was 1.9 percent greater than design.

2. Six-stage total efficiency was 0.66 at the design blade-jet speed ratio of 0.125, while weight flow was 2.4 percent over the design value.

3. Operation of the complete eight-stage unit showed total and static efficiencies of 0.67 and 0.65 at the design blade-jet speed ratio of 0.110. Weight flow was 2.7 percent above the design flow rate. The differences between these efficiencies and the design figures of 0.75 and 0.72 result from differences between the eight-stage turbine and the turbines on which the design efficiencies were based. These differences include interstage stator losses, the relative size of rotor-blade tip clearance, and relative blade trailing-edge flow blockage.

4. Examination of stage and overall performance at design turbine operation showed some deviation from the design equal work split because of variations in stage efficiency. The first stage operated at a total efficiency of 0.68, while all other stages operated near 0.60. This difference resulted largely from the differences in stator operation and a higher rotor-blade surface diffusion in the last six stages.

5. The variation in generalized torque with blade-jet speed ratio was nearly linear for all stage groups tested. The principal deviation from this occurred near zero speed, where torque parameters fell above the straight-line variation.

CONCLUDING REMARKS

Experimental performance testing of the eight-stage turbine showed an appreciable difference between experimental efficiency and the design or predicted efficiency. Examination of the experimental results, design features of the subject turbine, and reference information shows some reasons for this difference.

Efficiency assumptions used in the design of the eight-stage turbine were based on experimental performance of research turbines that were somewhat different in character. The reference research turbines were single-stage machines of 0.6 to 0.7 hub-tip radius ratios with very small rotor-blade tip clearances. These differences can account for a lower efficiency level in turbines of the type reported herein through the different ratios of tip clearance to passage height, blade trailing-edge blockage, and interstage stator flow conditions.

E-1454

Examination of the design characteristics of the subject turbine, experimental results, and reference information indicates several means by which efficiency could be improved. They are as follows:

1. Change the tip clearance from the elimination of blade material to a clearance recessed in the outer wall with rotor blades of full passage height.

2. Design the turbine stages for a higher efficiency level in the first stage than in the others in order to account for the lower losses associated with the first stator compared with subsequent stators.

3. Minimize blade trailing-edge blockage by using lower aspect ratios with minimum trailing-edge thickness.

4. Design the rotor blading with higher solidity and consequently lower blade-surface diffusion in order to reduce rotor losses.

A further gain in efficiency could be obtained by increasing the number of stages in order to decrease stage work and thereby increase stage blade-jet speed ratios.

Lewis Research Center
National Aeronautics and Space Administration
Cleveland, Ohio, November 2, 1961

REFERENCES

1. Rohlik, Harold E., and Crouse, James E.: Analytical Investigation of the Effect of Turbopump Design on Gross-Weight Characteristics of a Hydrogen-Propelled Nuclear Rocket. NASA MEMO 5-12-59E, 1959.

2. Rohlik, Harold E.: Investigation of Eight-Stage Bleed-Type Turbine for Hydrogen-Propelled Nuclear Rocket Applications. I - Design of Turbine and Experimental Performance of First Two Stages. NASA TM X-475, 1961.

E-1454

3. Stewart, Warner L.: Analytical Investigation of Multistage-Turbine Efficiency Characteristics in Terms of Work and Speed Requirements. NACA RM E57K22b, 1958.

4. Kofskey, Milton G.: Experimental Investigation of Three Tip-Clearance Configurations over a Range of Tip Clearance Using a Single-Stage Turbine of High Hub- to Tip-Radius Ratio. NASA TM X-472, 1961.

5. Stewart, Warner L.: Torque-Speed Characteristics for High-Specific-Work Turbines. NACA TN 4379, 1958.

[redacted]

TABLE I. - STAGE GROUP PERFORMANCE AT DESIGN SPEED AND OVERALL PRESSURE RATIO

(a) Overall stage group performance

Number of stages	Design pressure ratio, p_i'/p_e	Equivalent flow, $\frac{w\sqrt{\theta_{cr}}}{\delta}\epsilon$, lb/sec	Experimental pressure ratio, p_i'/p_e	Equivalent specific work, $\Delta h'/\theta_{cr}$, Btu/lb	Total efficiency, η
2	1.73	0.380	1.78	11.33	0.64
4	3.10	.380	3.40	21.60	.62
6	6.06	.380	6.62	32.84	.65
8	13.25	.380	13.25	42.80	.67

(b) Two-stage group performance

Stages	Two-stage work, $\Delta h'/\theta_{cr}$, Btu/lb	Two-stage total efficiency, η
1 and 2	11.33	0.64
3 and 4	10.27	.57
5 and 6	11.24	.62
7 and 8	9.96	.60

E-1454

[redacted]

E-1454

Figure 1. - Eight-stage turbine rotor.

[redacted]

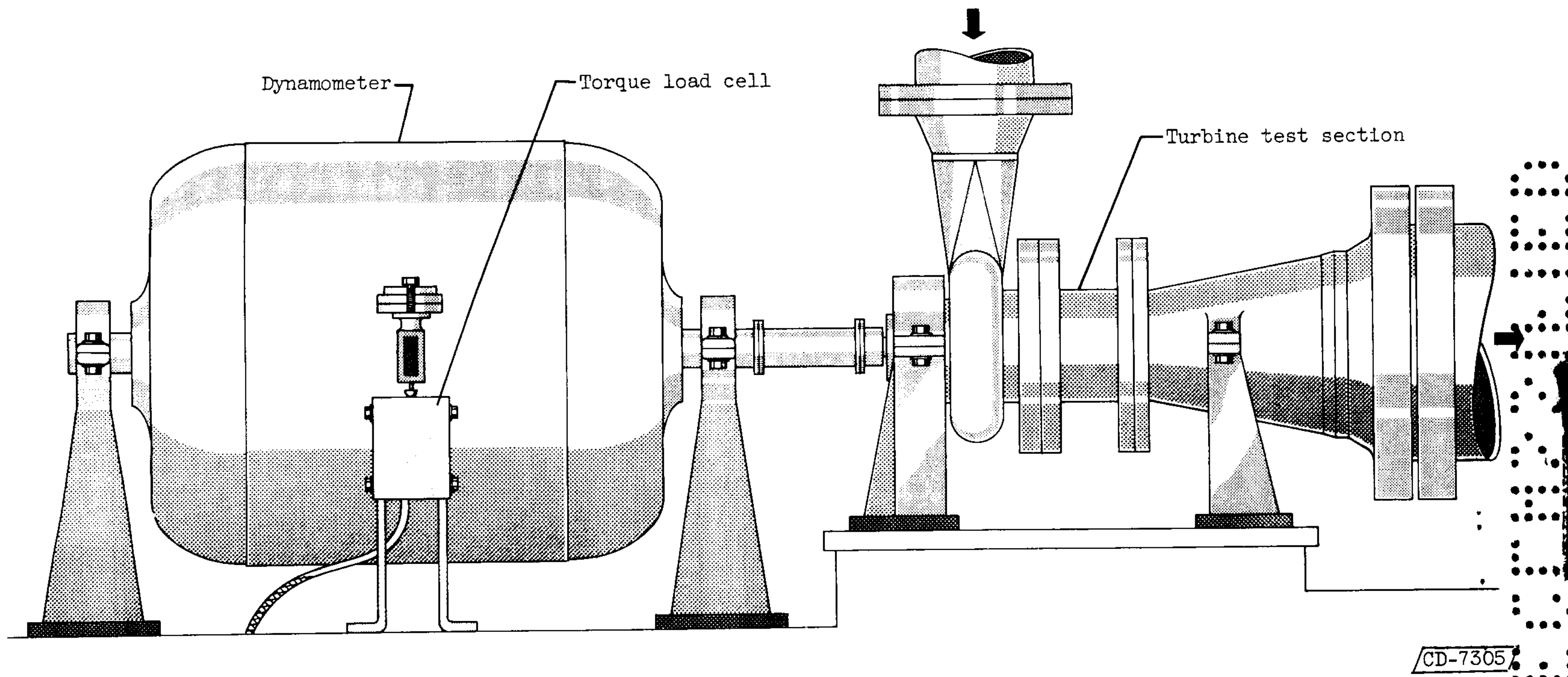

(a) Overall view.

Figure 2. - Turbine test rig.

[redacted]

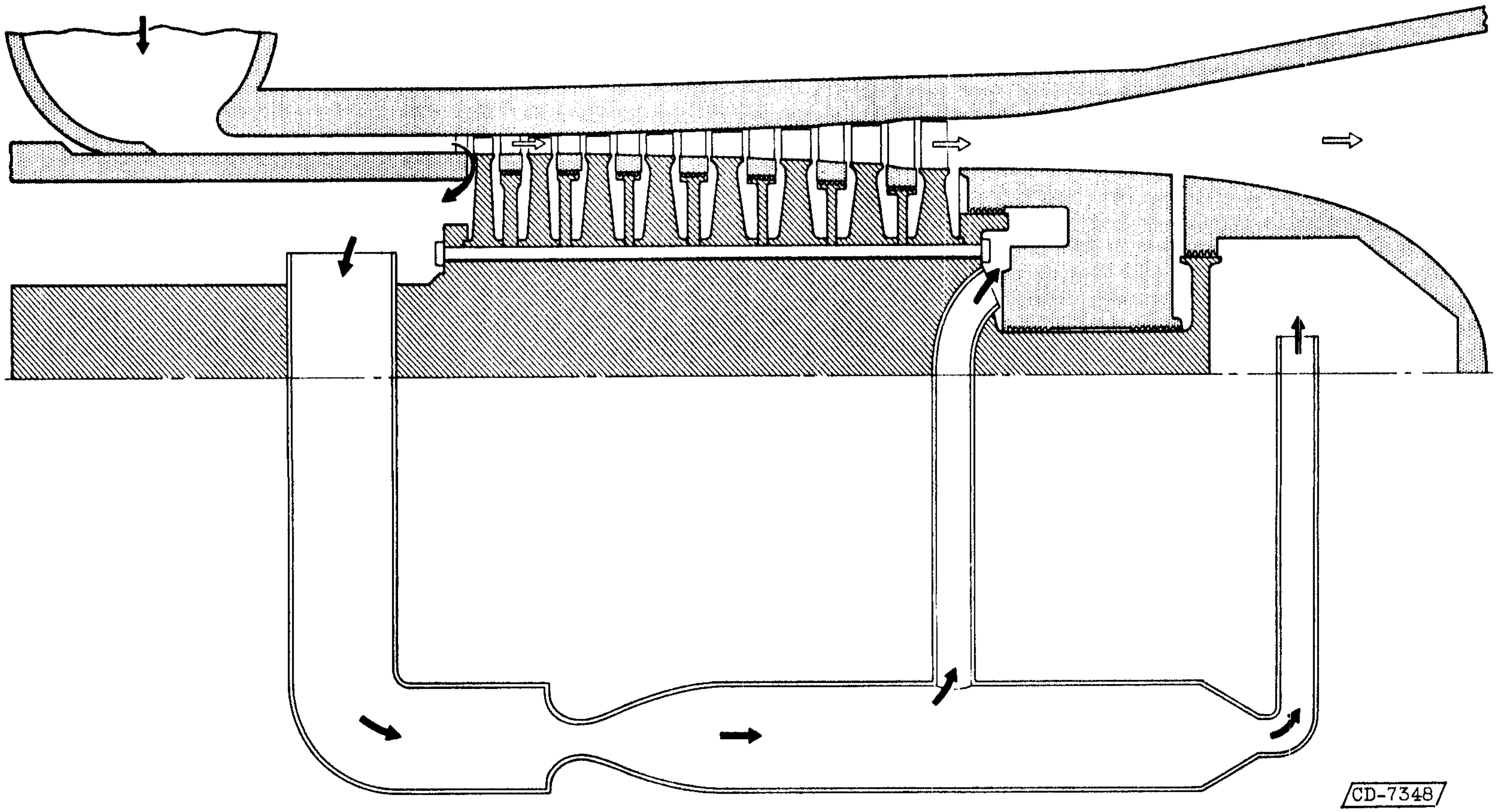

(b) Thrust balance system.

Figure 2. - Concluded. Turbine test rig.

[redacted]

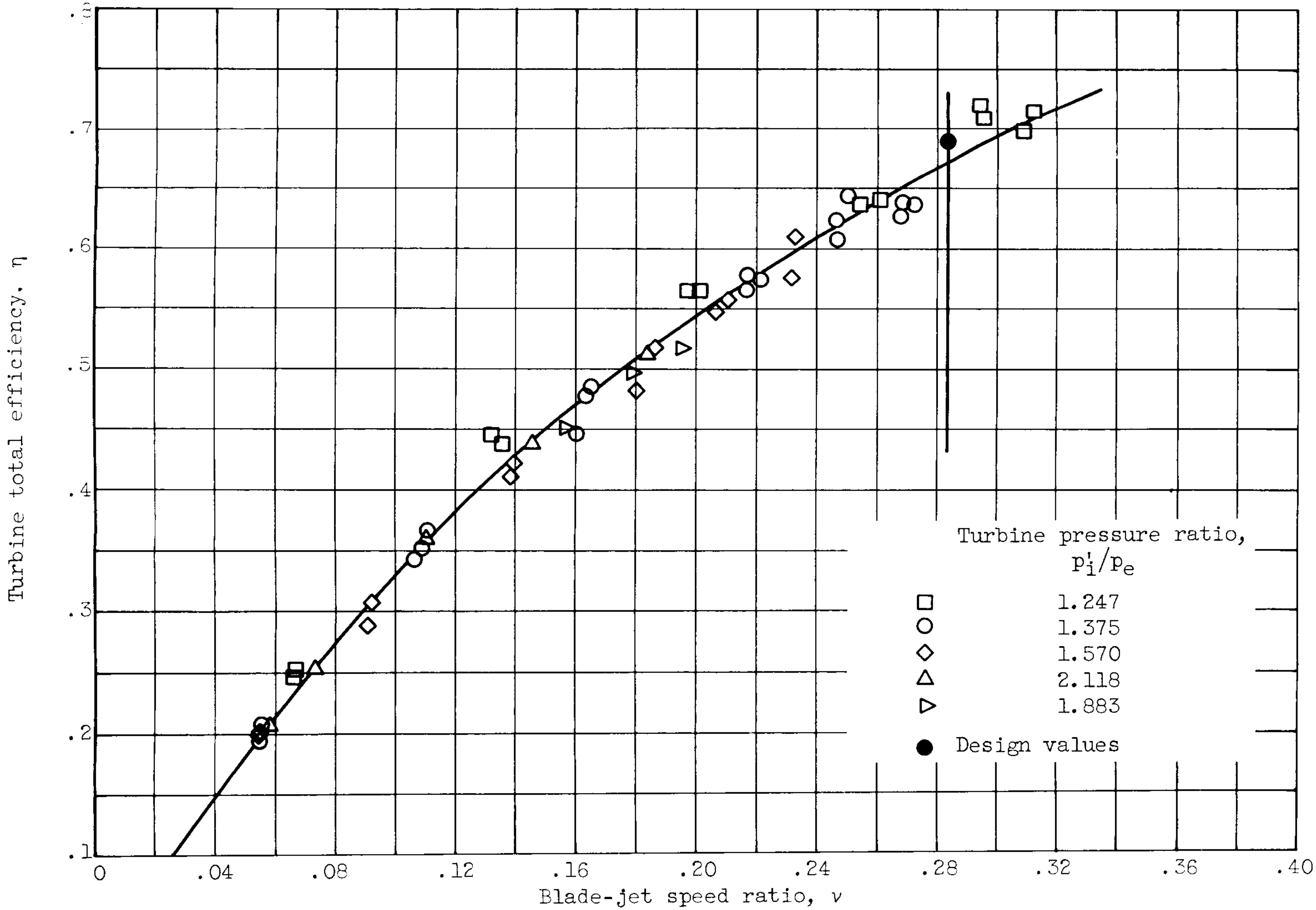

(a) First stage.

Figure 3. - Variation in total efficiency with blade-jet speed ratio.

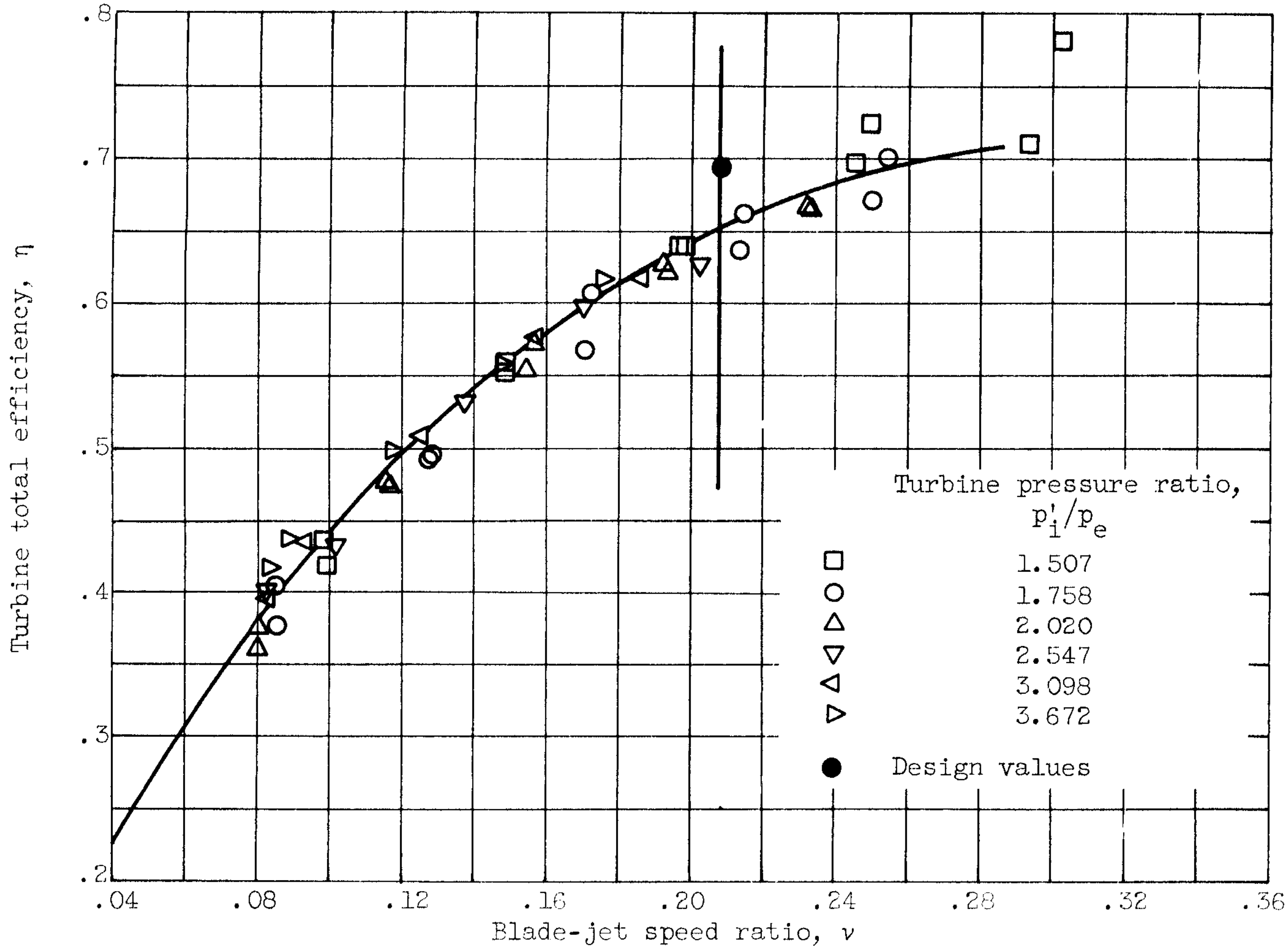

(b) First two stages.

Figure 3. - Continued. Variation in total efficiency with blade-jet speed ratio.

[redacted]

[redacted]

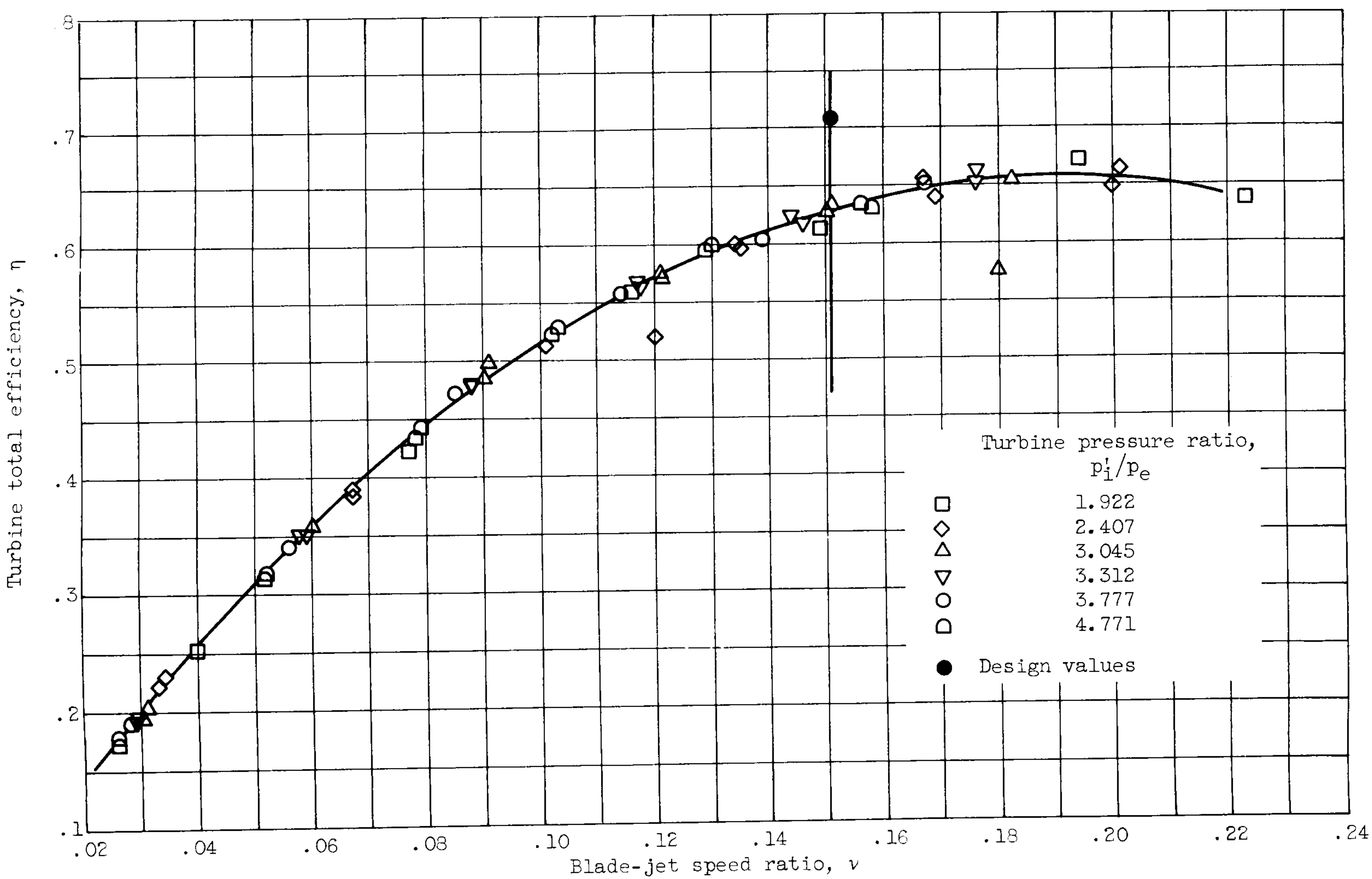

(c) First four stages.

Figure 3. - Continued. Variation in total efficiency with blade-jet speed ratio.

[redacted]

E-1454

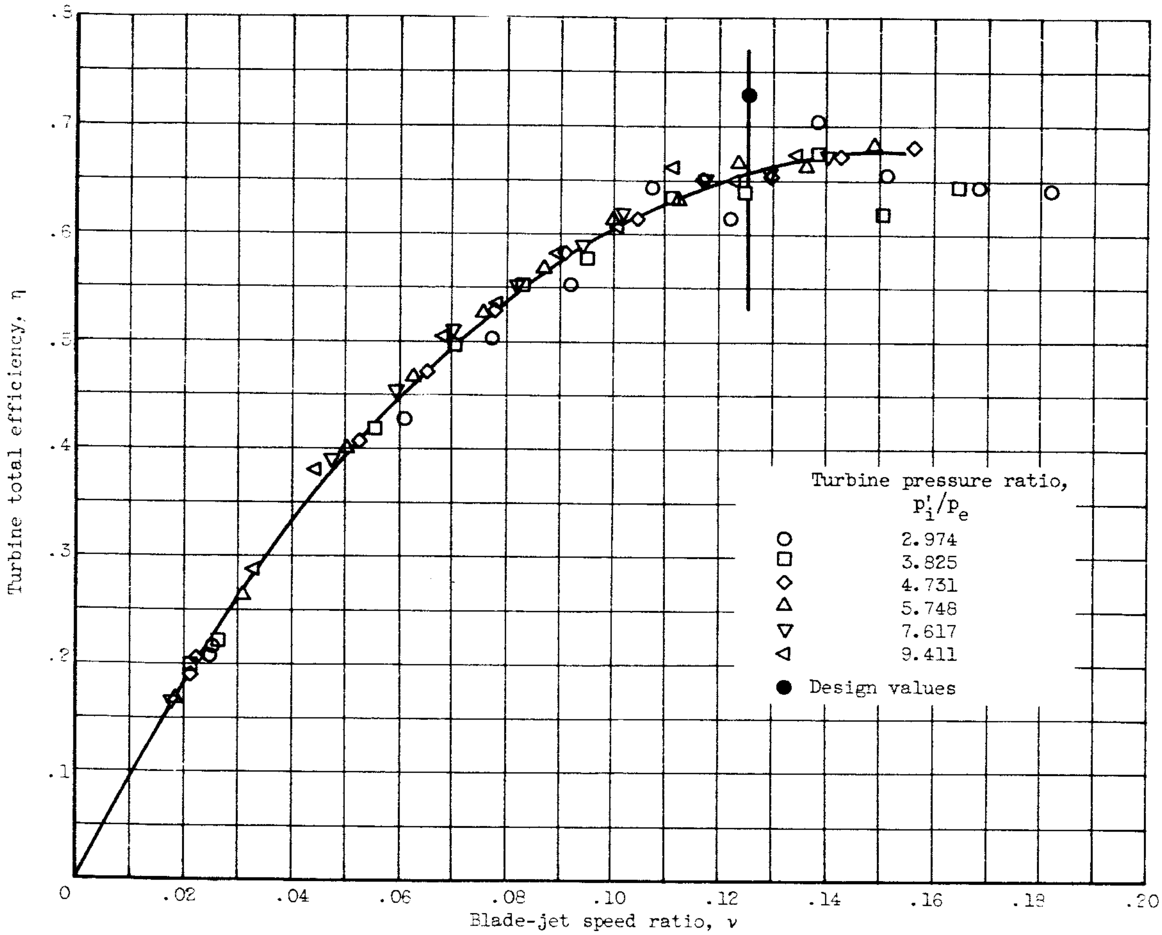

(d) First six stages.

Figure 3. - Continued. Variation in total efficiency with blade-jet speed ratio.

[redacted]

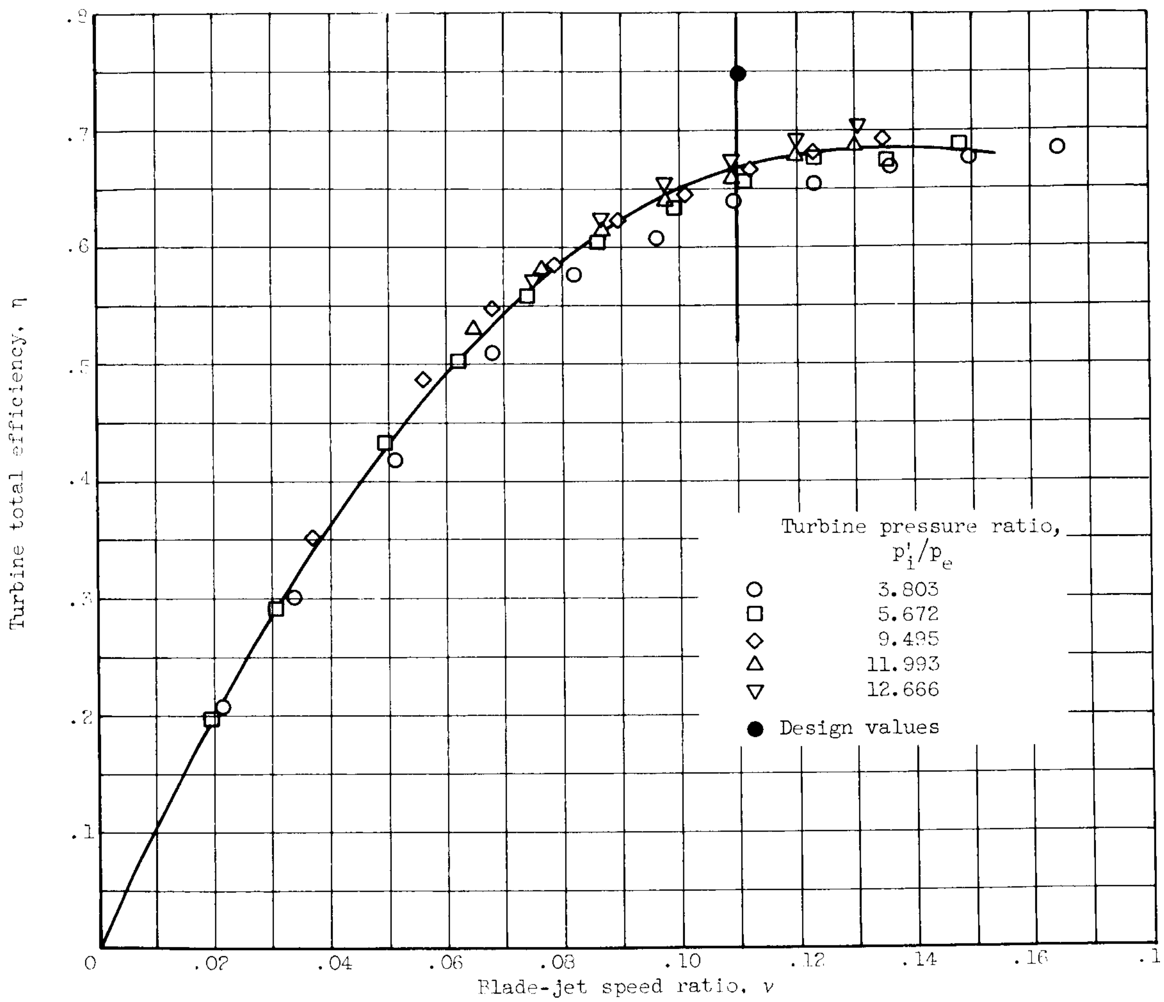

(e) All eight stages.

Figure 5. - Concluded. Variation in total efficiency with blade-jet speed ratio.

[redacted]

E-1454

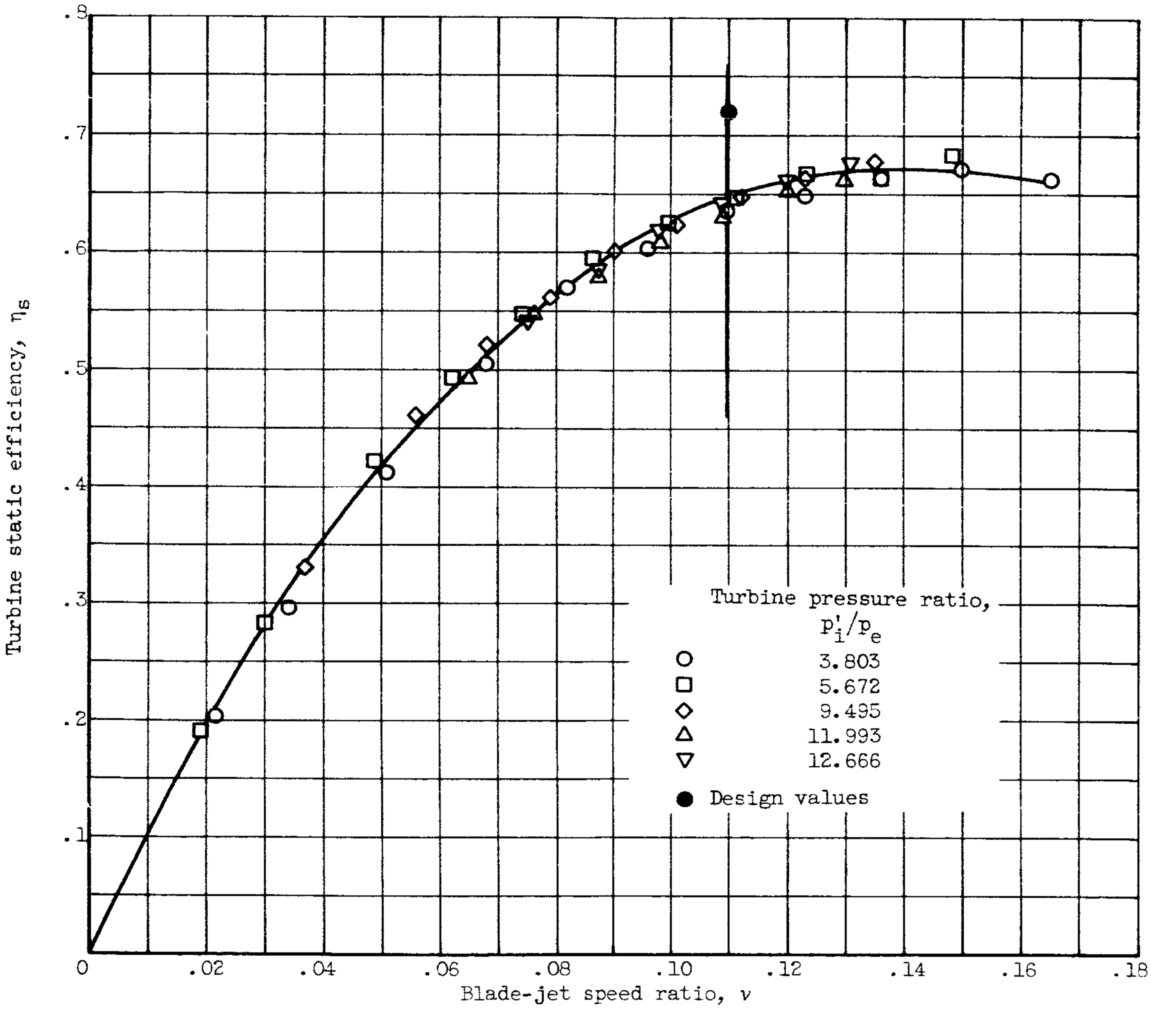

Figure 4. - Static efficiency variation of eight-stage turbine.

DECLASSIFIED [redacted]

E-1454

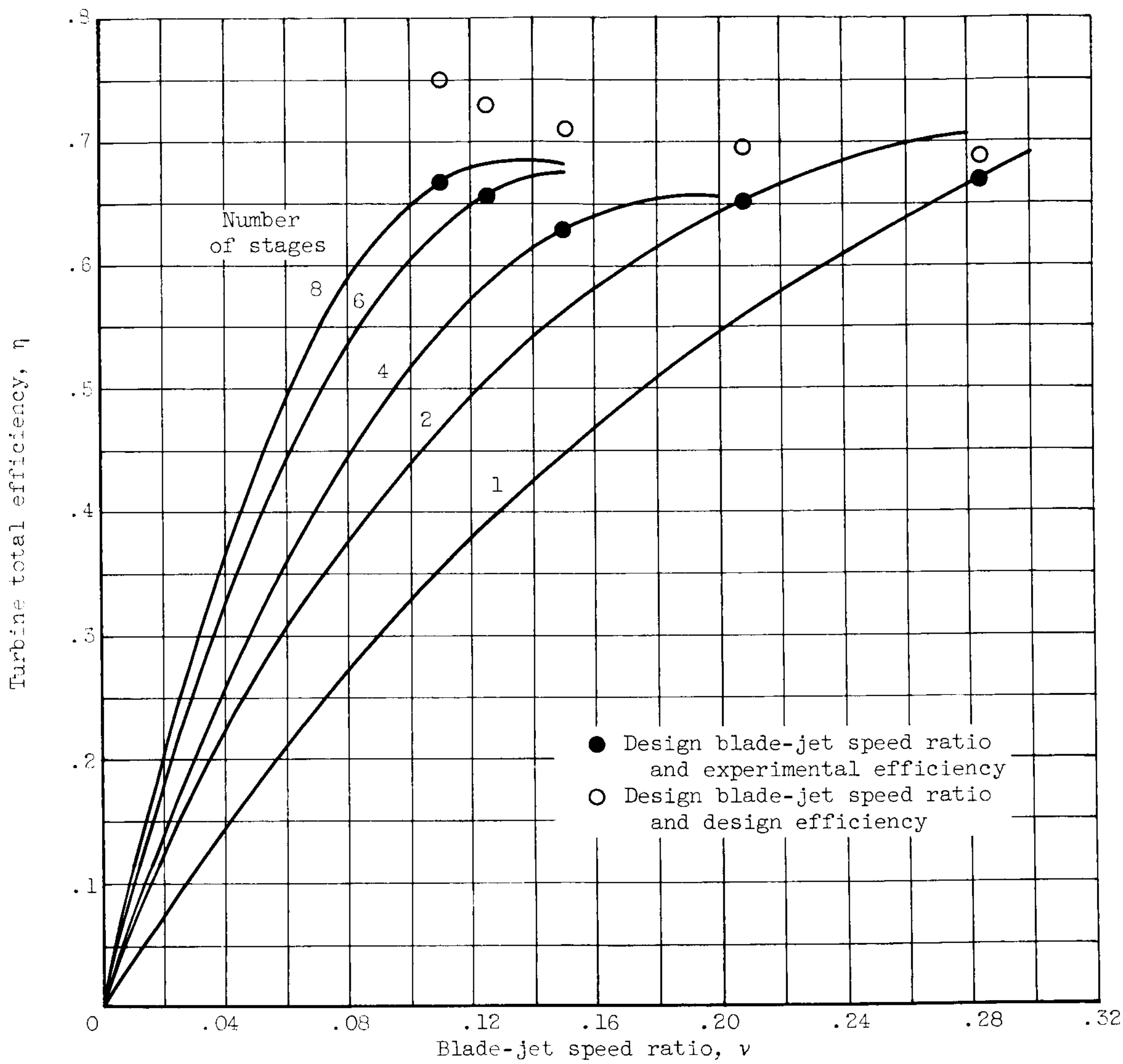

Figure 5. - Variation in total efficiency with blade-jet speed ratio for all stage groups tested.

[redacted]

[redacted]

E-1454

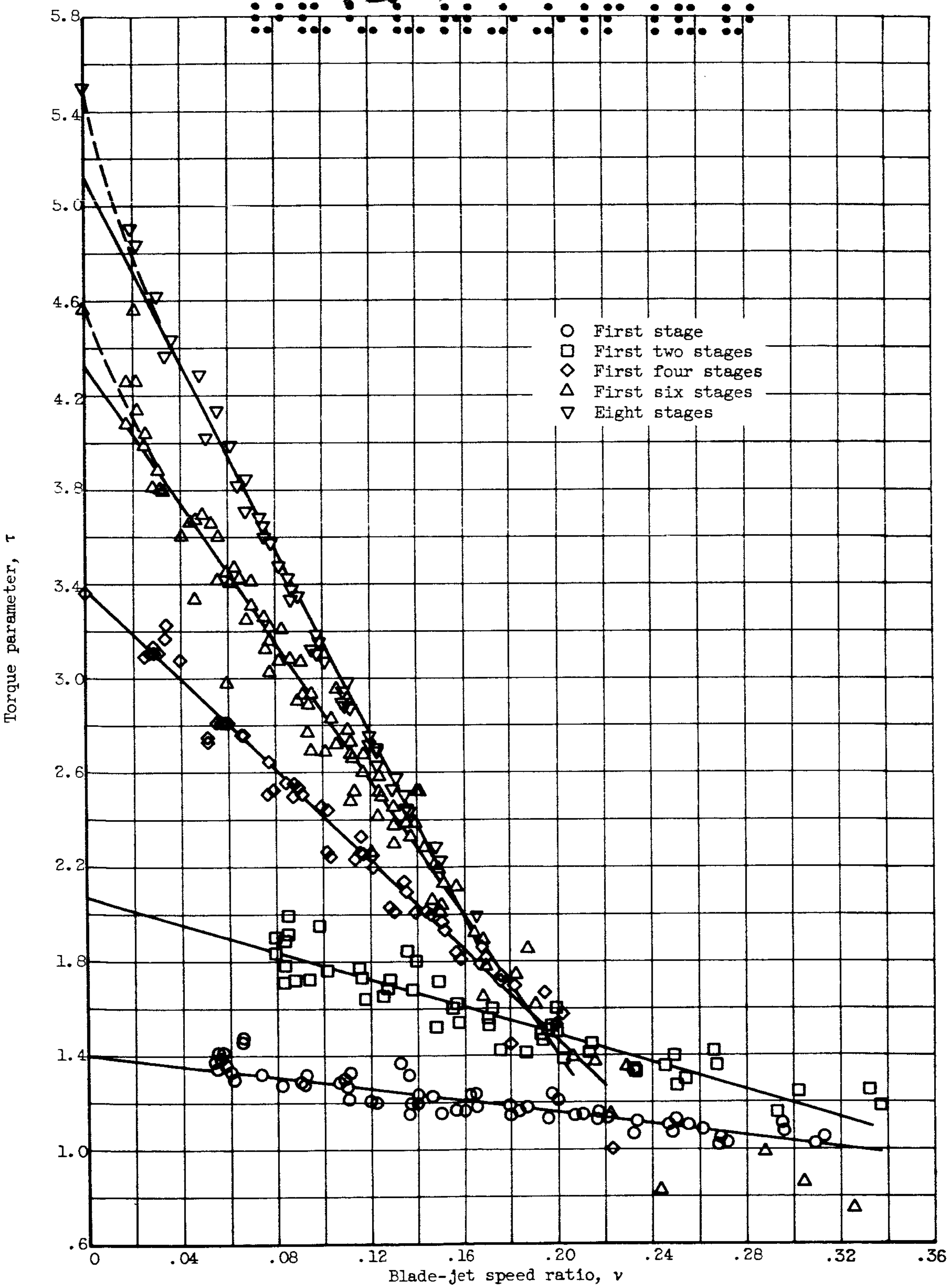

Figure 6. - Variation of torque parameter with blade-jet speed ratio.

[redacted]

E-1454

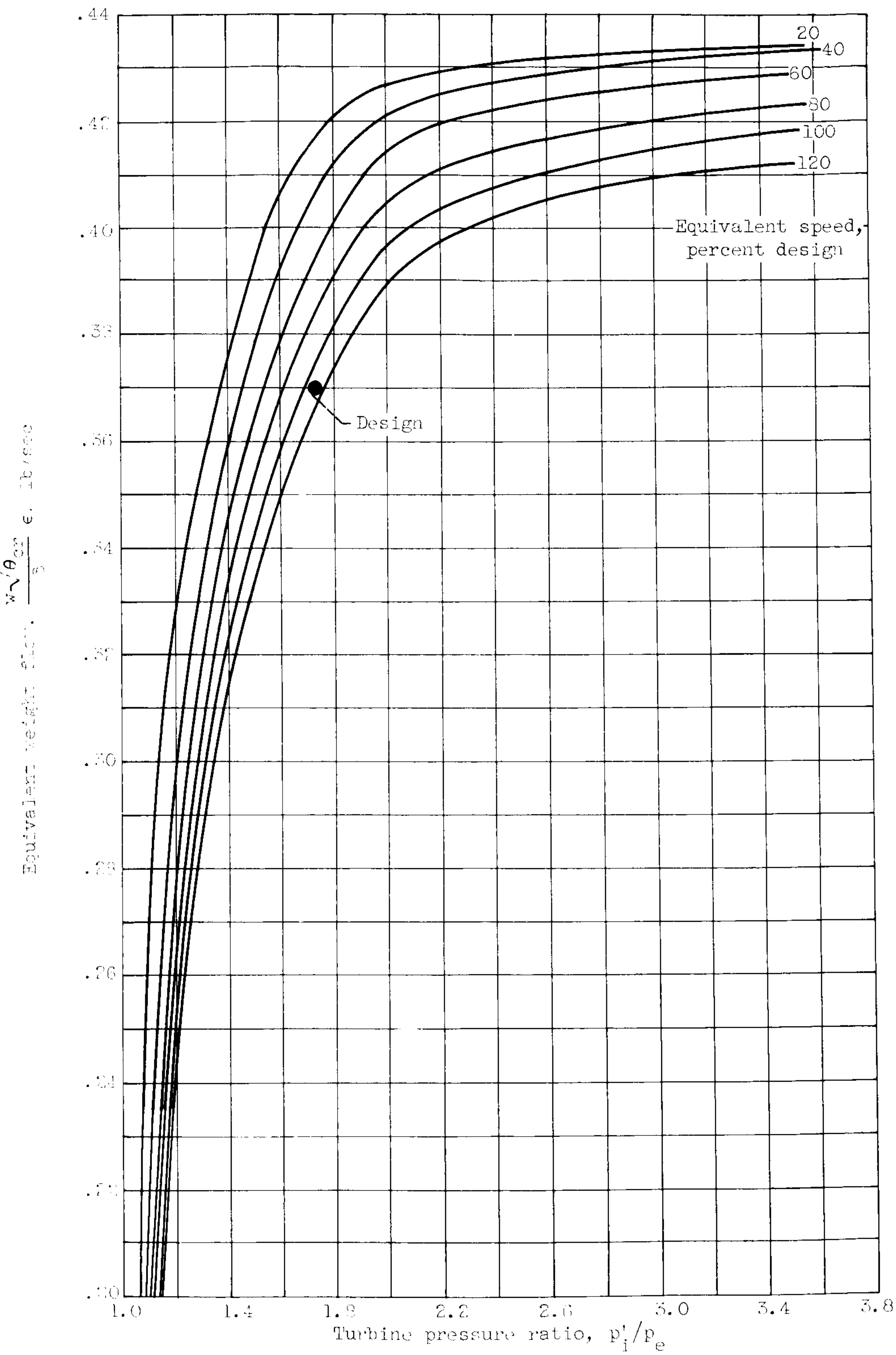

(a) First two stages.

Figure 7. - Variation in equivalent flow with pressure ratio.

[redacted]

E-1454

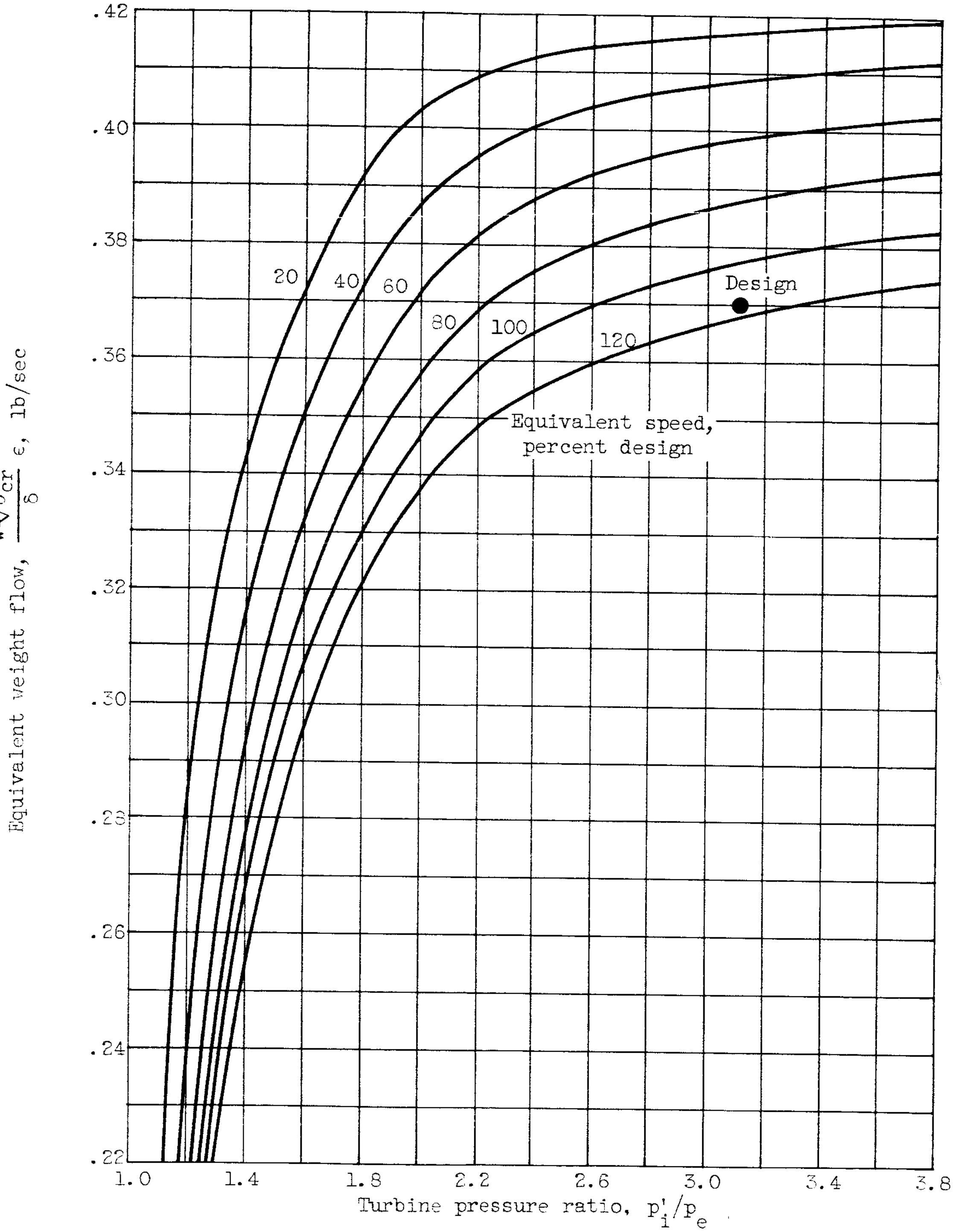

(b) First four stages.

Figure 7. - Continued. Variation in equivalent flow with pressure ratio.

[redacted]

E-1454

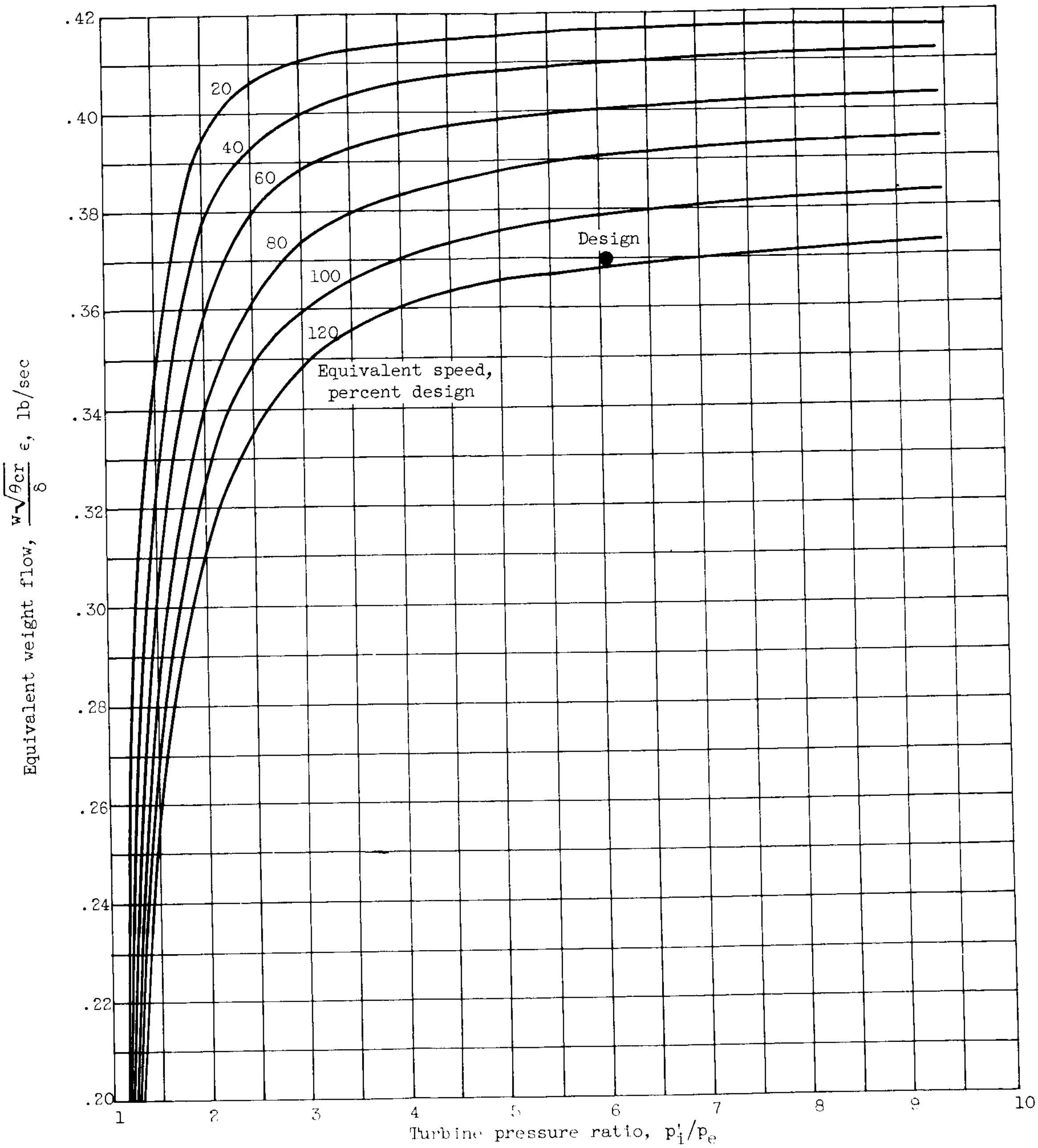

(e) First six stages.

Figure 7. - Continued. Variation in equivalent flow with pressure ratio.

[redacted]

E-1454

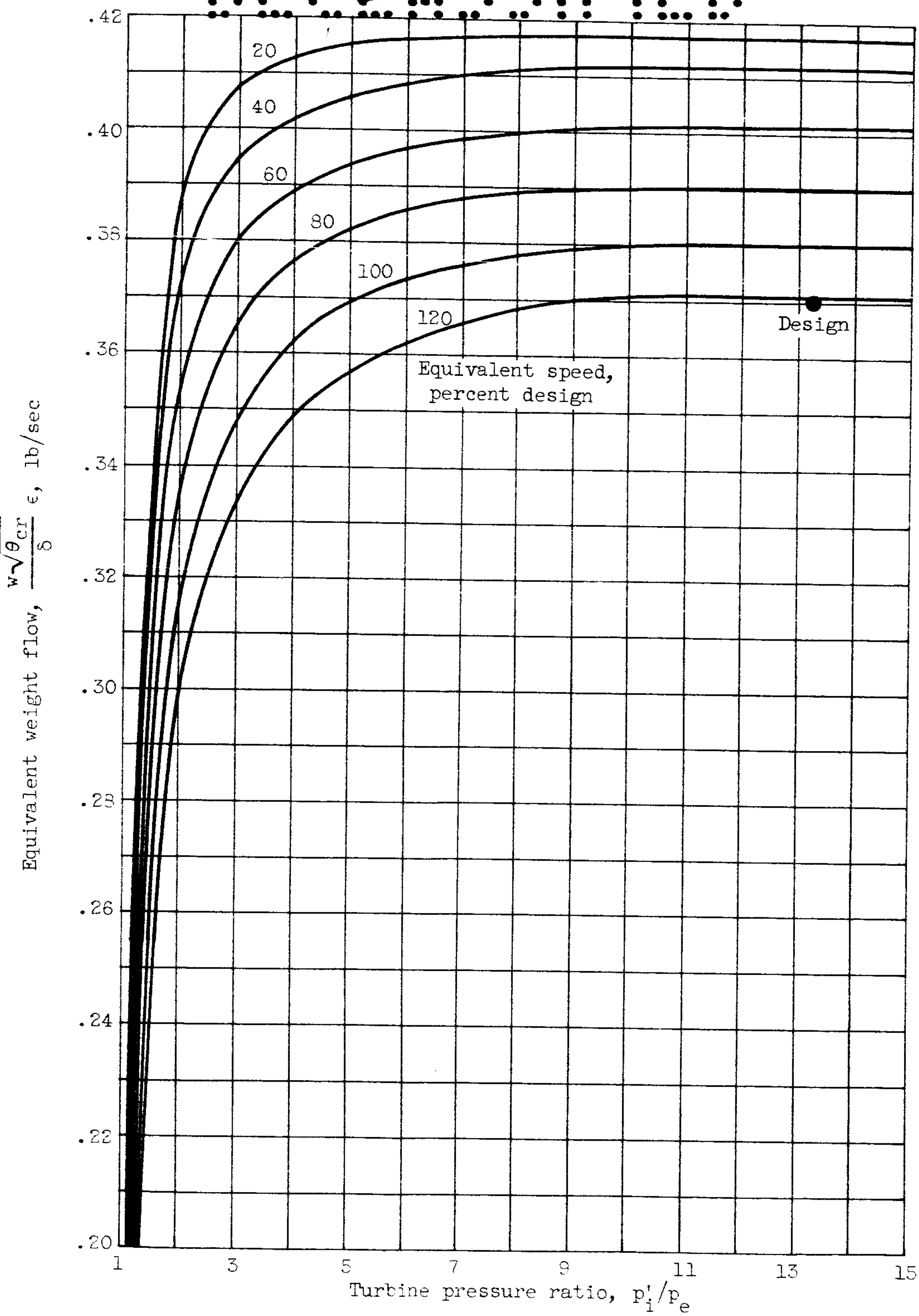

(d) Eight-stage turbine.

Figure 7. - Concluded. Variation in equivalent flow with pressure ratio.

[redacted]

E-1454

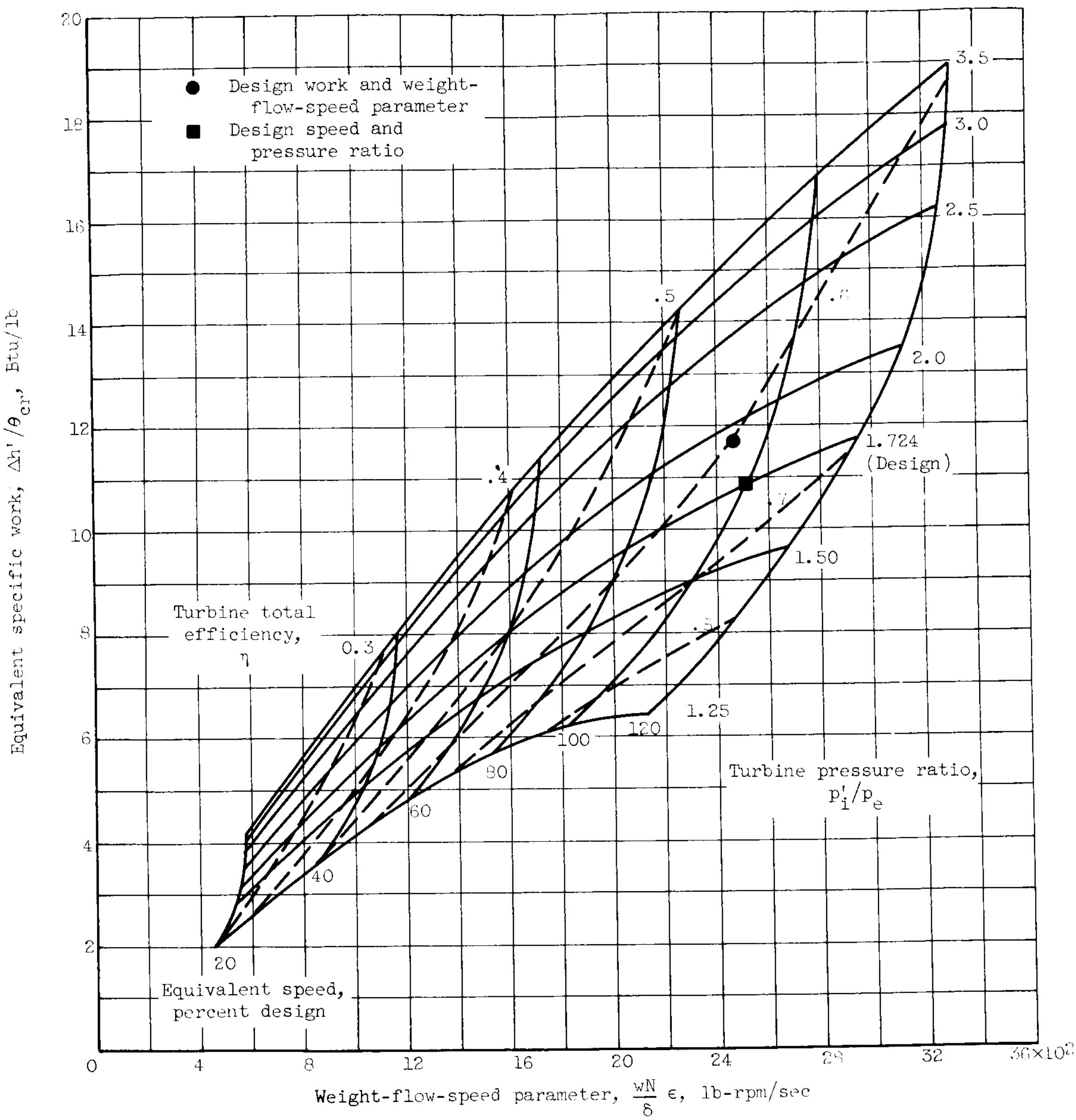

(a) First two stages.

Figure 8. - Turbine performance.

[redacted]

E-1454

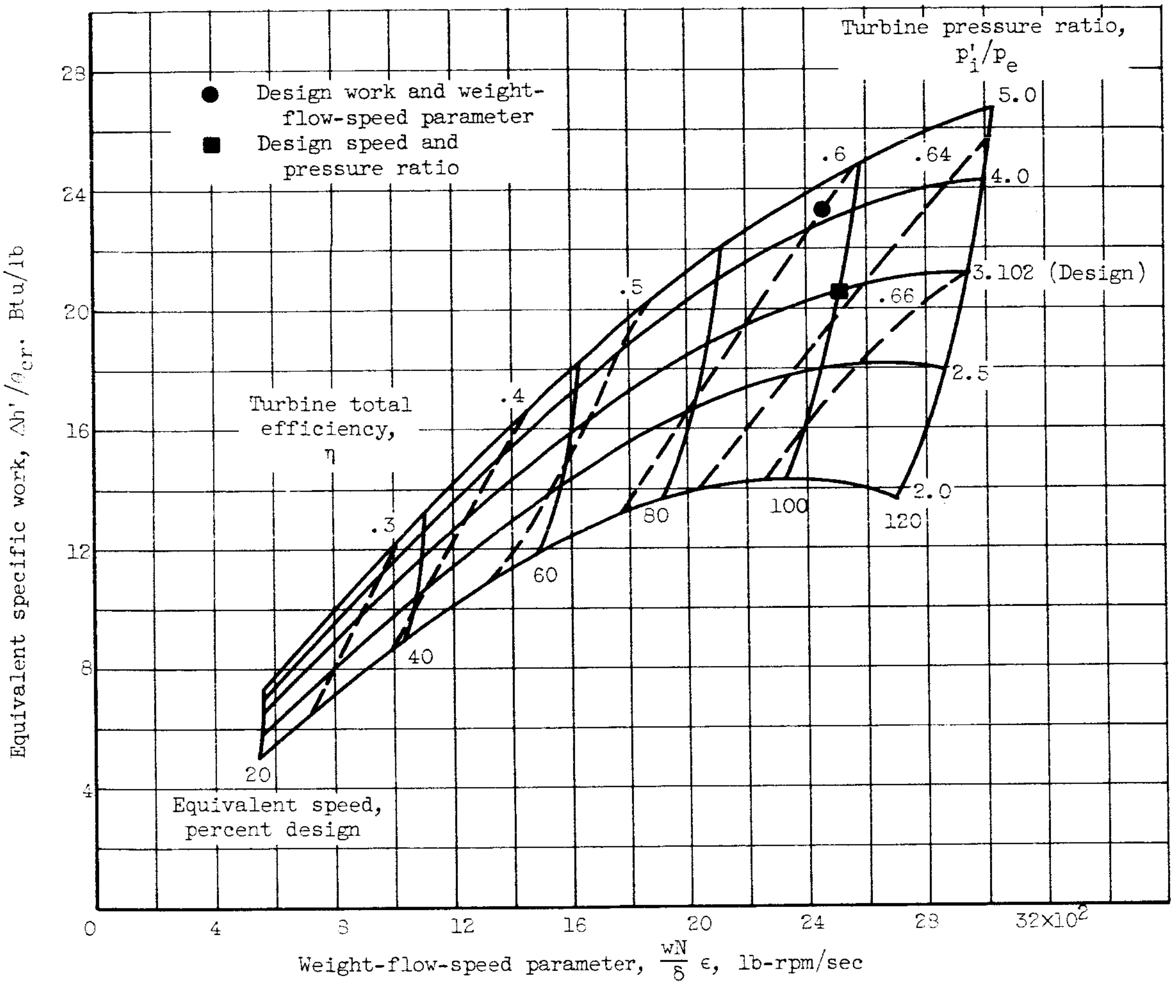

(b) First four stages.

Figure 8. - Continued. Turbine performance.

[redacted]

E-1454

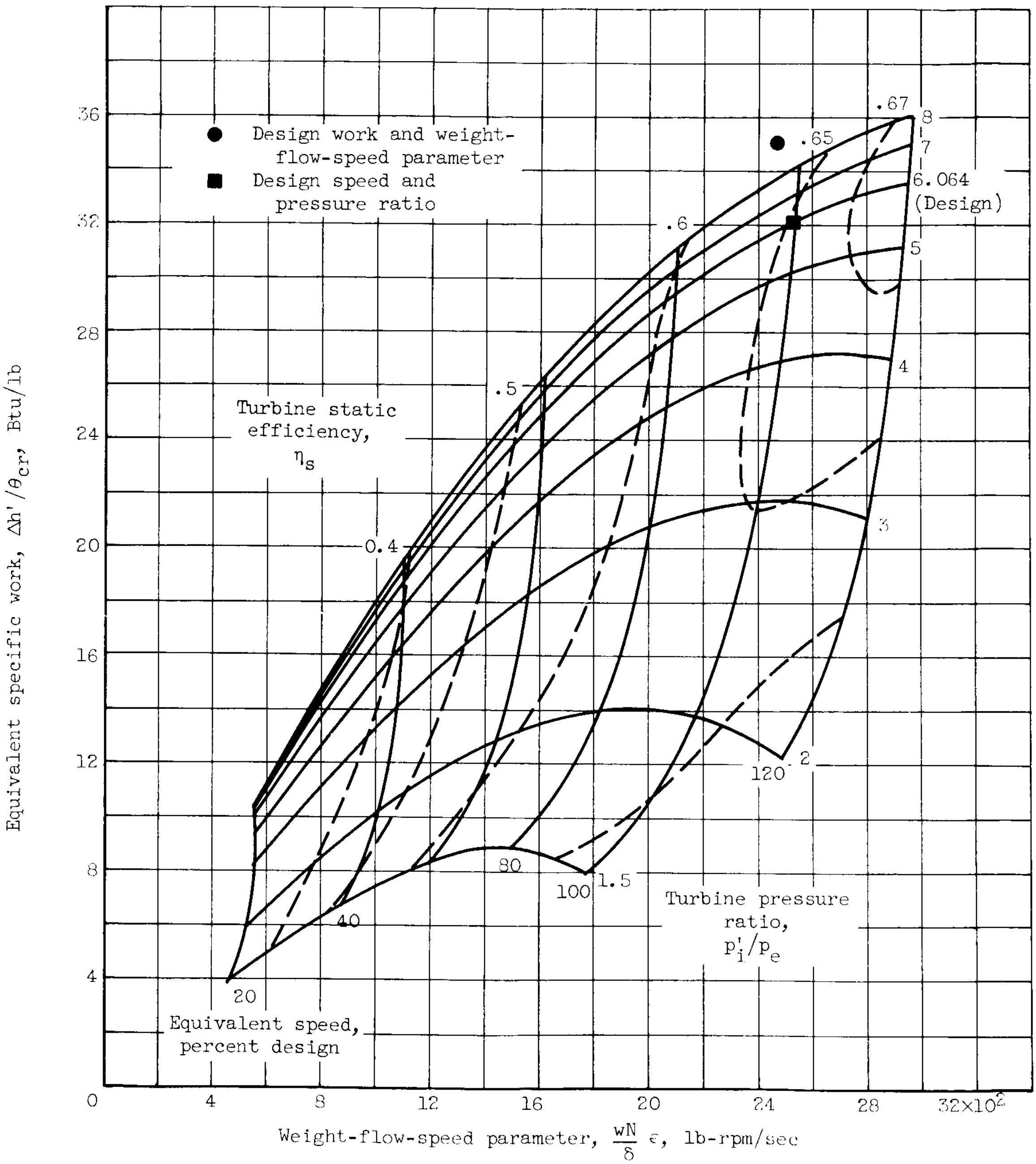

(c) First six stages.

Figure 8. - Continued. Turbine performance.

[redacted]

[redacted]

E-1454

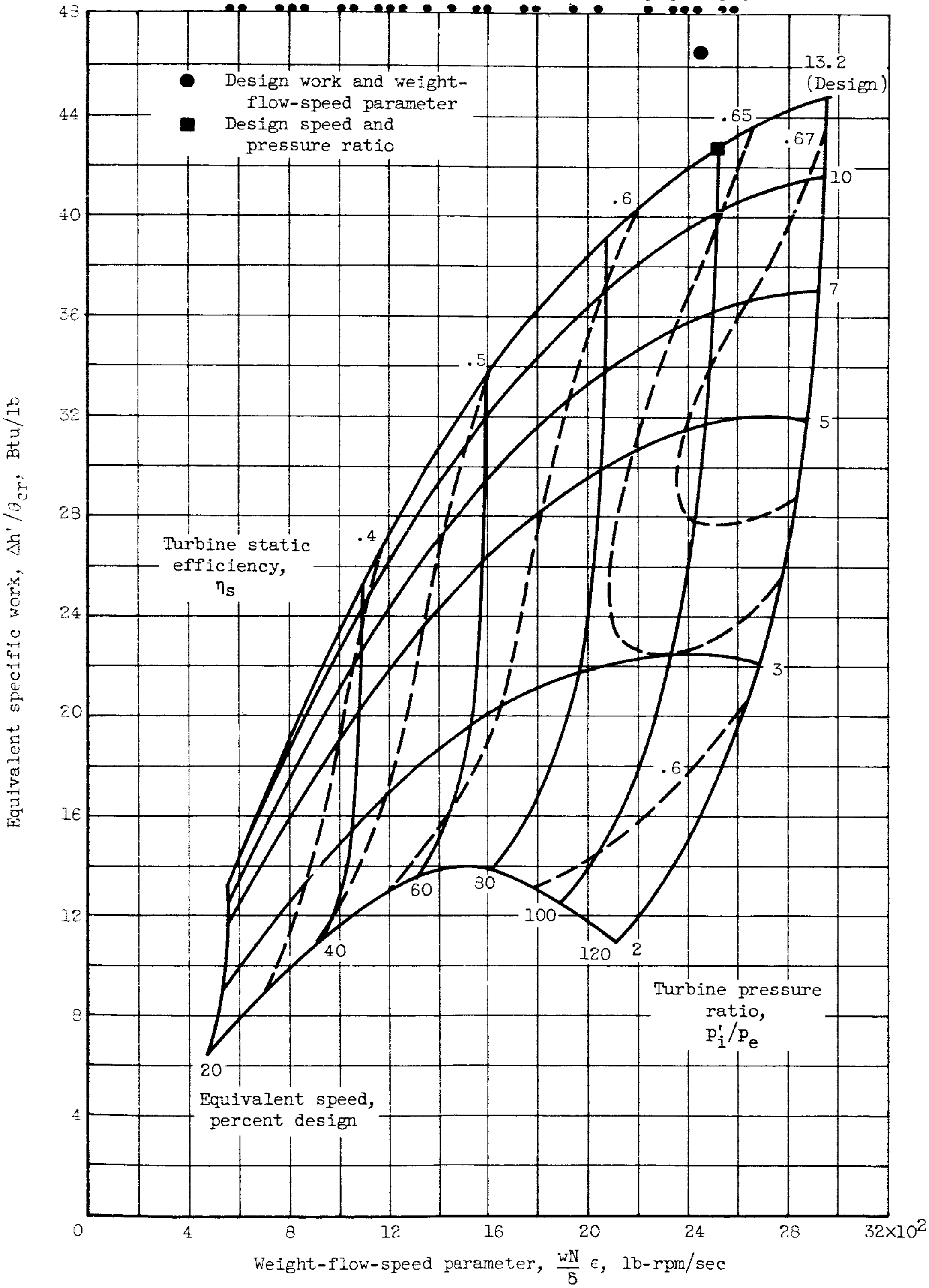

(d) Eight-stage turbine

Figure 8. - Concluded. Turbine performance.